

Cross-section sensitivity analyses of 14 MeV Neutron Benchmark Experiment on Tungsten

I. Kodeli *

OECD NEA-Data Bank, 12 Bd des Iles, 92130 Issy-les-Moulineaux, France

Abstract

The 14 MeV Neutron Experiment on Tungsten carried out at the Frascati Neutron Generator (FNG) in 2002 was analysed using deterministic computational tools, with a stress on the cross-section sensitivity analysis. The DORT discrete ordinates (S_N) with FENDL-2 and JENDL-3.3 cross-section data, and the SUSD3D sensitivity and uncertainty computer codes were used in the analysis. The sensitivity profiles of various reaction rates measured at four positions up to 35 cm in the block of tungsten, and covering thermal to fast neutron energy range, with respect to all the partial as well as the total cross-sections of tungsten were calculated using the SUSD3D code. Combined with the comparison of the calculated and the measured reaction rates, the cross-section sensitivity profiles indicate areas where further evaluation work is needed. The results were compared with those obtained from the OKTAVIAN Tungsten Experiment and FNS Clean Experiment on the Tungsten Cylindrical Assembly.

© 2004 Elsevier B.V. All rights reserved.

1. Introduction

The Neutron Experiment on tungsten was performed at the Frascati Neutron Generator (FNG) in 2002 with the objective of determining the state-of-the-art of the tungsten nuclear data files for the use in fusion reactor applications. This experiment complements the information obtained from the OKTAVIAN Tungsten Experiment and FNS Clean Experiment on Tungsten Cylindrical Assembly.

The shielding block is made of layers of DENSI-MET-180 and -176, containing 95.0 and 92.3 wt% of tungsten, respectively. The block had the height of 46.85 cm, a width varying between 42 and 47 cm, and a thickness of 49 cm. The 14 MeV FNG neutron source was located 5.3 cm in front of the block. Several neutron reaction rates, covering fast and thermal neutron energies, and gamma heating were measured at four positions along the central beam axes of the block, at approximately 5, 15, 25 and 35 cm in the W block. The

results of the experimental measurements as well as the comparison with the MCNP-4C calculations are included in [1].

This work was performed in the scope of the European Fusion Technology Programme of the EC and the SINBAD project. The descriptions of the FNG, OKTAVIAN and FNS Tungsten benchmarks and the analyses are available in the SINBAD database of the OECD/NEA.

2. S_N transport calculations

The present report demonstrates the analysis using discrete ordinates (S_N) deterministic transport codes, including the sensitivity and uncertainty analysis. The DORT [2] S_N , and the SUSD3D [3] sensitivity and uncertainty computer codes were used in the analysis. S_{16} , P_5 approximation and first collision source method of the GRTUNCL code were applied in the DORT calculations. The multigroup cross-sections were taken from the FENDL-2 [4] and JENDL-3.3 [5] libraries, and the detector response functions from the IRDF-90.2 [6]

* Tel.: +33-1 45 24 10 74; fax: +33-1 45 24 11 28.

E-mail address: ivo.kodeli@oecd.org (I. Kodeli).

Table 1
Calculated reaction rates using the DORT code with FENDL-2 (FEN-2) and JENDL-3.3 (J-3.3) cross-sections compared with the measurements along the central mock-up axis

Detector position → Reaction ↓	5 cm			15 cm			25 cm			35 cm						
	E (%)	C/E	ΔC ^a (%)	E (%)	C/E	ΔC ^a (%)	E (%)	C/E	ΔC ^a (%)	E (%)	C/E	ΔC ^a (%)				
		FEN-2 J-3.3		FEN-2 J-3.3		FEN-2 J-3.3		FEN-2 J-3.3		FEN-2 J-3.3		FEN-2 J-3.3				
⁹³ Nb(n,2n)	1.88E-4 ± 4.0	0.94	0.95	0.9	1.04E-5 ± 5.0	0.96	1.04	0.9	9.95E-7 ± 5.0	0.87	1.01	0.9	1.08E-7 ± 6.0	0.81	1.01	0.8
⁸⁸ Ni(n,2n)	1.49E-5 ± 4.0	0.93	0.95	1.9	8.15E-7 ± 4.5	0.91	1.00	1.8	7.19E-8 ± 5.5	0.85	1.00	1.6	1.76E-7 ± 6.0	0.75	0.94	0.8
⁹⁰ Zr(n,2n)	3.06E-4 ± 4.4	0.98	1.00	0.9	1.76E-5 ± 5.0	0.92	1.00	0.9	1.57E-6 ± 5.5	0.86	1.00	0.8	2.78E-8 ± 6.5	0.85	1.05	0.4
²⁷ Al(n,α)	4.45E-5 ± 4.0	0.97	0.99	0.5	2.72E-6 ± 5.0	0.94	1.02	0.4	2.53E-7 ± 6.0	0.90	1.04	0.4	2.91E-8 ± 6.4	0.77	0.95	1.3
⁵⁶ Fe(n,p)	4.56E-5 ± 5.0	0.93	0.94	1.5	2.79E-6 ± 5.0	0.89	0.96	1.4	2.62E-7 ± 5.5	0.84	0.96	1.4	1.35E-7 ± 5.5	0.96	1.05	7.3
⁸⁸ Ni(n,p)	1.58E-4 ± 4.5	1.04	1.00	10.8	1.16E-5 ± 5.5	1.03	1.02	8.7	1.14E-6 ± 5.5	1.04	1.07	7.8				
¹¹⁵ In(n,n')	1.38E-4 ± 4.6	0.91	0.82	1.9	1.50E-5 ± 5.5	0.94	0.79	2.0	1.67E-6 ± 5.7	1.02	0.82	2.1				
¹⁹⁷ Au(n,γ)	6.23E-4 ± 4.0	1.02	1.13	0.7	2.98E-4 ± 4.0	1.03	1.18	0.7	1.03E-4 ± 4.0	1.05	1.20	0.7	2.84E-5 ± 5.5	1.10	1.23	0.7
⁵⁵ Mn(n,γ)	1.67E-5 ± 5.0	1.59	1.73	56	8.74E-6 ± 5.0	1.50	1.76	79	3.30E-6 ± 5.5	1.48	1.72	87	1.04E-6 ± 6.4	1.42	1.60	89

For the energy ranges covered by different detectors see Fig. 2.

^a ΔC, the calculational uncertainty, takes into account only the uncertainties in the detector response functions (IRDF-90.2 evaluation).

evaluation. For the ¹⁹⁷Au(n,γ) reaction, the self-shielded detector response function was used, taking into account the actual thickness of 0.05 mm of the detector foil. The self-shielding was found to be very important, and results in a reduction of the calculated reaction rate by almost a factor of 2 with respect to the infinite diluted case.

The exact description of the geometry composed of layers of DENSIMET-180 and -176 with slightly different shapes would require detailed 3D modelling using codes like TORT or THREEDANT. As the uncollided and first collision module for TORT (GRTUNCL-3D) was not available the experimental model was described in a slightly simplified, but representative 2-D cylindrical geometry. The model included 33 radial and 75 axial intervals.

The comparison of the measured and the calculated neutron reaction rates at the four detector positions is shown in Table 1. The DORT results are in excellent agreement, within 5%, with the MCNP/4C calculations, presented in [1]. Comparing the calculations with the experiment it seems that the FENDL-2 library tends to underestimate the fast neutron flux, by more than 20% at the depth of 35 cm in W. ⁵⁸Ni(n,p), ⁵⁸In(n,n') and ¹⁹⁷Au(n,γ), covering lower energies, are within 1–2σ of the experimental error bars. The situation is reversed for the JENDL-3.3 data where good agreement was found for the fast reactions, but for the epithermal and thermal reactions the discrepancies are of about 20%.

These results are consistent with those obtained from the OKTAVIAN Tungsten and FNS Clean Experiment on Tungsten Cylindrical Assembly. Measured and calculated spectra from the FNS Tungsten experiment are shown in Fig. 1.

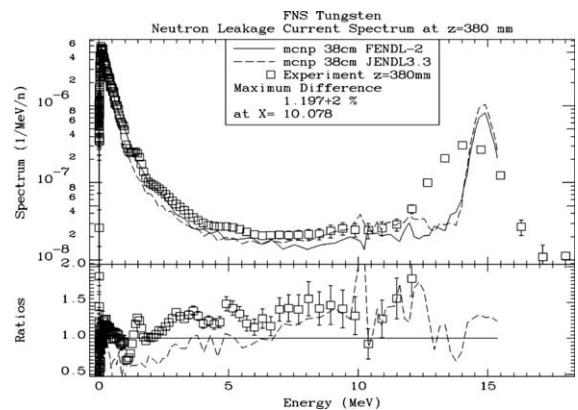


Fig. 1. Comparison of the measured and calculated spectra in the FNS Tungsten experiment (38 cm in W). Calculations were performed with MCNP4C code using the FENDL-2 and JENDL-3.3 cross-sections. E/C ratios are shown.

3. Sensitivity (and uncertainty) analysis

The cross-section sensitivity and uncertainty analyses were performed using the SUS3D 3] code, which calculates the sensitivity profiles from the direct and adjoint angular moment fluxes obtained by the S_N codes. The code was widely used in the past in several EFF projects (like FNG bulk shield and SiC benchmarks [7,8]), as well as for fission reactor and benchmark analyses.

The sensitivity of the reaction rates with respect to the variations of the nuclear transport cross-sections of tungsten and the response functions were studied. The sensitivities with respect to the detector response functions are presented in Fig. 2, indicating the energy ranges covered by the detectors. Examples of sensitivity profiles with respect to the transport cross-sections of tungsten are shown in Figs. 3–5 and the energy-integrated sensitivities are presented in Table 2. These re-

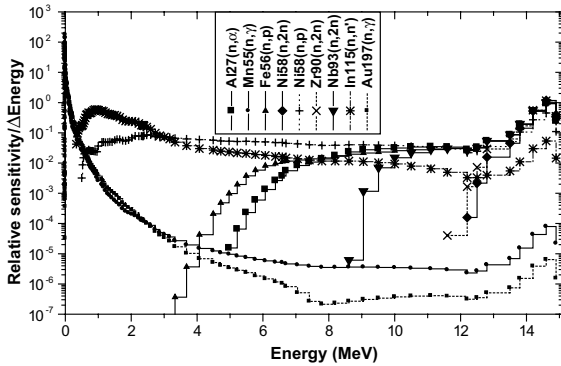


Fig. 2. Sensitivity to the detector response functions (direct sensitivity term) at the detector position 4 (35 cm in W block). The energy ranges covered by different detectors can be seen (e.g. for Au and Mn ~ 1 keV to few 100 keV, for In ~ 0.5 to few MeV, etc.).

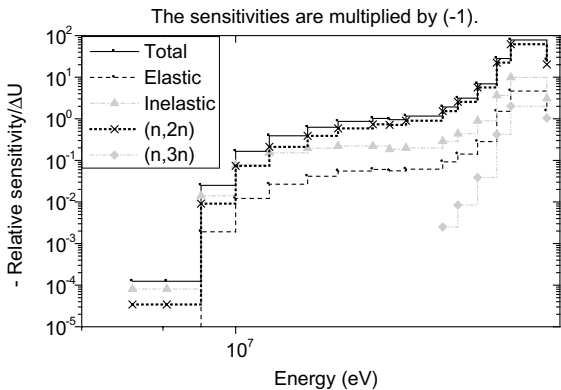


Fig. 3. Sensitivity of the $^{93}\text{Nb}(n,2n)$ reaction rate at deepest detector position (35 cm) to the W cross-sections.

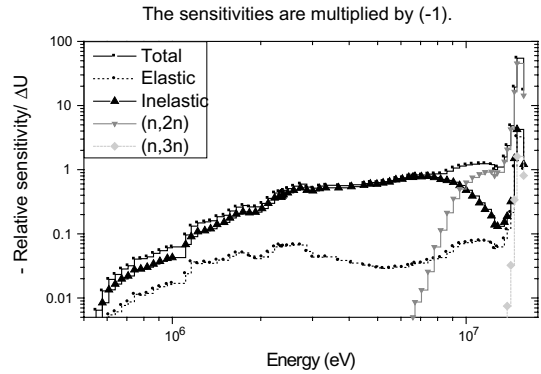


Fig. 4. Sensitivity of the $^{58}\text{Ni}(n,p)$ reaction rate at deepest detector position (35 cm) to the W cross-sections.

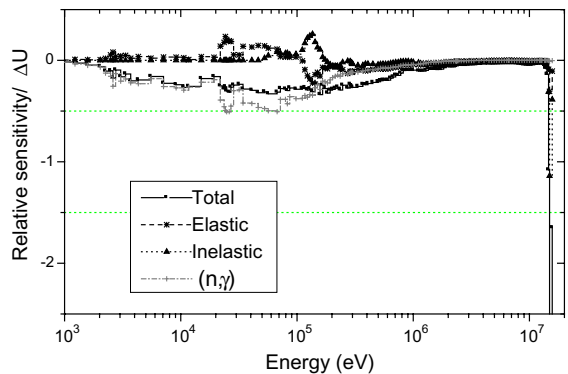


Fig. 5. Sensitivity of the $^{197}\text{Au}(n,\gamma)$ reaction rate at the deepest detector position (35 cm) to the W cross-sections.

sults indicate that by far the most important cross-section reaction on W in the fast energy range is (n,2n). At lower energies, covered by the $^{58}\text{Ni}(n,p)$ and $^{115}\text{In}(n,n')$ dosimetry reactions (above ~2 MeV), the inelastic and the elastic scattering become increasingly important. The $^{197}\text{Au}(n,\gamma)$ and $^{55}\text{Mn}(n,\gamma)$ dosimetry reactions are on the other hand predominantly sensitive to the (n,γ) reaction. Taking into account the observed C/E values this gives indications on the reaction types and energy ranges requiring further studies.

The uncertainty of a target quantity is determined by folding the sensitivity profiles with the covariance matrices, therefore both the information on the sensitivity with respect to the basic parameters, as well as the corresponding covariance matrices must be known. The covariance information related to the detector response functions was taken from the IRDF-90.2 evaluation. On the other hand, no cross-section covariance data for tungsten are available at present in any evaluation and the complete uncertainty analysis was therefore not possible.

Table 2

Integral sensitivities of the detector responses with respect to the tungsten cross-section, for the deepest position in the tungsten block (35 cm)

Cross-section reaction	Sensitivity (%/%)						
	$^{93}\text{Nb}(n,2n)$	$^{90}\text{Zr}(n,2n)$	$^{27}\text{Al}(n,\alpha)$	$^{58}\text{Ni}(n,p)$	$^{115}\text{In}(n,n')$	$^{197}\text{Au}(n,\gamma)$	$^{55}\text{Mn}(n,\gamma)$
Total	-4.52	-4.48	-4.52	-4.54	-4.42	-1.81	-1.58
Elastic	-0.26	-0.28	-0.25	-0.30	-0.58	+0.01	+0.19
Inelastic	-0.59	-0.65	-0.61	-1.34	-2.29	-0.06	+0.04
(n,2n)	-3.55	-3.43	-3.53	-2.80	-1.41	-0.15	-0.13
(n,3n)	-0.11	-0.12	-0.11	-0.09	-0.06	+0.006	+0.006
(n, γ)	-0.002	-0.002	-0.002	-0.011	-0.071	-1.60	-1.70
(n,p)	-0.007	-0.007	-0.007	-0.006	-0.004	-0.002	-0.002
(n,d)	-0.001	-0.001	-0.001	-0.001	-0.001	-4E-4	-3E-4
(n, α)	-0.003	-0.003	-0.003	-0.002	-0.002	-8E-4	-8E-4

The uncertainties in the reaction rates due to the uncertainties in the detector response functions are given in Table 1, together with the corresponding C/E values. This already permits the high discrepancy in the $^{55}\text{Mn}(n,\gamma)$ reaction rates to be explained, which seems to be due to the uncertainties in the resonance energies between 1 and 100 keV of this response function in the IRDF-90.2 evaluation. For the other reactions the uncertainty is of the order of few percentage, up to 10% for the $^{58}\text{Ni}(n,p)$ reaction.

4. Conclusions

Confirming the previous experience from other FNG benchmark experiment analyses [7,8] the DORT/GRT-UNCL and SUSD3D transport, sensitivity and uncertainty code system proved to be well established for this type of transport analysis. The agreement between the DORT and the MCNP results is better than 5%.

DORT (and MCNP) results indicate that FENDL-2 underestimates the fast neutron reaction rates (above ~ 6 MeV), by 20–30% at the depth of 35 cm in tungsten. Excellent agreement, within the experimental errors, was obtained using the JENDL3.3 data. The most important neutron reaction in this energy range in W was found to be (n,2n), respectively 5-times and 10–15-times more important than the inelastic and elastic cross-sections.

At lower energies, covered by the $^{58}\text{Ni}(n,p)$ and $^{115}\text{In}(n,n')$ detectors (above ~ 2 MeV), the inelastic and elastic scattering become increasingly important. The $^{197}\text{Au}(n,\gamma)$ and $^{55}\text{Mn}(n,\gamma)$ reactions are on the other hand predominantly sensitive to the (n, γ) reaction. The $^{58}\text{Ni}(n,p)$, $^{115}\text{In}(n,n')$ and $^{197}\text{Au}(n,\gamma)$ reaction rates calculated using FENDL2 agree with the measurements within 1σ of the experimental error bars. JENDL-3.3 on the other hand respectively under- and over-predicts the $^{115}\text{In}(n,n')$ and $^{197}\text{Au}(n,\gamma)$ reaction rates by over 20%. High discrepancy was found in $^{55}\text{Mn}(n,\gamma)$ due to the

uncertainty in the IRDF-90.2 response function in the resonance range.

Similar trends were observed from the analysis of the OKTAVIAN and FNS W benchmarks.

Due to the lack of information on the tungsten cross-section covariance data, the uncertainty analysis could be performed only partially, covering only the uncertainties related to the response functions. Nevertheless the above sensitivity results already give indications on the reaction types and energy ranges requiring further studies and improvements.

References

- [1] P. Batistoni, M. Angelone, L. Petrizzi, M. Pillon, Neutronics Benchmark Experiment on Tungsten, these Proceedings.
- [2] W.A. Rhoades et al., DOORS 3.2, One-, two-, three-dimensional discrete ordinates neutron/photon transport code system, CCC-650, Radiation Safety Information Computational Center, Oak Ridge National Laboratory, 1998.
- [3] I. Kodeli, Nucl. Sci. Eng. 138 (2001) 45.
- [4] H. Wienke, M. Herman, FENDL/MG-2.0 and FENDL/MC-2.0, The processed cross-section libraries for neutron-photon transport calculations, version 1 of February 1998, IAEA-NDS-176, Rev.1, International Atomic Energy Agency, Vienna, 1998 (Data retrieved on-line from the IAEA Nuclear Data Section).
- [5] K. Kosako, N. Yamano, T. Fukahori, K. Shibata, A. Hasegawa, The libraries FSXSLIB and MATXSLIB based on JENDL-3.3, JAERI-Data/Code 2003-011, 2003.
- [6] N.P. Kocherov, P.K. Mc Laughlin, The international reactor dosimetry file, IAEA-NDS-141, Rev. 2, Vienna, 1993.
- [7] I. Kodeli, L. Petrizzi, P. Batistoni, J. Nucl. Sci. Technol. (Suppl. 1) (2000) 713.
- [8] Y. Chen, U. Fischer, I. Kodeli, R.L. Perel, A. Angelone, P. Batistoni, L. Petrizzi, M. Pillon, K. Seidel, S. Umholzer, Fus. Eng. Des. 69 (2003) 437.